Polymer Journal, Vol. 18, No. 11, pp 819—836 (1986)

Effects of Stereoregularity on Molecular Parameters of Polyacrylonitrile Polymerized by Gamma-Ray Irradiation

Kenji KAMIDE, Hitoshi YAMAZAKI, and Yukio MIYAZAKI

Fundamental Research Laboratory of Fibers and Fiber-Forming Polymers, Asahi Chemical Industry Company, Ltd., Takatsuki, Osaka 569, Japan

(Received March 17, 1986)

ABSTRACT: Polyacrylonitrile (referred to as γ-PAN) was prepared by γ-ray irradiation on an acrylonitrile–urea canal complex at −78°C. The pentad tacticity was evaluated from ^{13}C NMR spectra according to a method proposed by Kamide *et al.* The content of a *mmmm* sequence (*m*; meso) for γ-PAN was 0.37 ± 0.02 over a wide range of molecular weight, which was about 4.4 times larger than that for PAN, prepared by conventional redox polymerization (R-PAN). Light scattering and solution viscosity were measured in dimethyl sulfoxide (DMSO), 57—67 wt% aq nitric acid at 25°C. By extrapolation of the second virial coefficient A_2 to zero 56.5 wt% aq nitric acid was expected to be a Flory theta solvent at 25°C. Mark–Houwink–Sakurada equations and empirical relations between the radius of gyration $\langle S^2 \rangle_z^{1/2}$ and $\bar{M}_w$ were determined in various solvents. The unperturbed chain dimension A was determined by four methods. In DMSO γ-PAN has larger A than R-PAN. The conformation parameter σ was 2.6—2.8 for γ-PAN, which is some 35% larger than the expected value when simple steric hindrance due to the side chain group is considered. Unexpectedly larger conformation parameters σ for γ- and R-PAN were interpreted by considering the rigidity of the chain due to intra-interactions between neighbouring CN groups in meso-sequence.

KEY WORDS Polyacrylonitrile / Dilute Solution Property / Light Scattering / Mark–Houwink–Sakurada Equation / Unperturbed Chain Dimension / Conformation Parameter / γ-Ray Irradiation / Urea–Canal Complex / Stereoregularity /

Since the latter 1950's, numerous studies have been carried out on the effects of stereoregularity on the molecular characteristics of polymers in solutions.[1-23] The results obtained can be summarized in short as: (1) The parameters K_m and a in the Mark–Houwink–Sakurada (MHS) equation,

$$[\eta] = K_m M^a \tag{1}$$

($[\eta]$, limiting viscosity number; M, molecular weight; K_m and a, parameters characteristic of the combination of polymer and solvent at a given temperature) are not significantly influenced by the stereoregularity of a polymer, if it is dissolved in a good solvent.[1,7,10,12,17,21,22] (2) The second virial coefficient A_2 becomes smaller even in a good solvent for a polymer with higher stereoregularity.[1,10,17] (3) The unperturbed chain dimension A (see eq 5) is larger for a polymer with higher stereoregularity and A of the isotactic polymer is usually larger than A of a syndiotactic polymer.[3,6-9,11,14,17,20-23] (4) A decreases with an increase in temperature.[1,2,4-6,20] These characteristic features of dilute solutions of stereoregular polymers were reviewed for example by Kamide (1962),[24] Krigbaum (1964)[25] and Cowie (1972).[26] Here, it should be noted that (1) in only less than half the above studies, the tacticities of the polymers were characterized by NMR and other methods as diad (poly(methyl methacrylate) (PMMA),[9] poly-

(1-pentene) (P1P)[20] and triad (poly(α-methyl styrene) (PαMS),[13-16] poly(isopropyl acrylate) (PIPA)[21,22]); (2) a highly stereospecific polymer has a tendency to form a gel or crystallize when dissolved in theta solvent and A for only a few polymers, such as PαMS,[13,15] poly(1-butene) (P1B),[18] and poly(vinyl acetate) (PVAc),[23] was determined directly from the unperturbed radius of gyration in the theta solvents by light scattering. (3) For many other polymers, the limiting viscosity number $[\eta]$ or the radius of gyration measured in good solvents was analyzed to estimate A.[2,9,14,16,20,22] Not much progress has been made for the last ten years.

As is well known, it is experimentally difficult to prepare polyacrylonitrile (PAN) with high stereoregularity and the effect of stereoregularity on the dilute solution properties of PAN has never been studied in detail. A few exceptions are works by Inagaki *et al.*[27] and by Kamide and his coworkers.[28] Inagaki *et al.* observed that MHS equations and accordingly, A, estimated from Stockmayer–Fixman plot (see eq 8), for PAN in dimethylformamide depend on polymerization temperature when a redox catalyst is used, concluding that the syndio-tacticity, as estimated from the peak at 950 cm^{-1} in infrared spectrum, might increase with decreasing polymerization temperature (−30 −60 °C). These predictions were not unfortunately confirmed with later NMR experiments by Matsuzaki *et al.*[29,30] Kamide, Kobayashi, and their collaborators[31] studied thermodynamic properties of PAN, polymerized using redox and non-redox catalysts in aqueous and non-aqueous media, noting that the MHS equation and A, estimated from the Stockmayer–Fixman plot (see eq 8) of the polymers polymerized using azobisisobutyronitrile in benzene, differ slightly, but significantly from those of polymers prepared under different conditions. The detailed structure of the ^1H NMR spectrum for these PAN sample are somewhat different, but no further analysis on the tacticity was made in their study. Kamide and Terakawa[28] who studied the polymer polymerized by irradiating γ-ray on an acrylonitrile–urea canal complex at low temperature (hereafter, referred to as γ-PAN), showed that the solubility of γ-PAN in DMF, a good solvent for PAN conventionally polymerized (hereafter referred as R-PAN), becomes extremely low. Unfortunately, in their work, the diad tacticity for γ-PAN was indirectly estimated by using Matsuzaki *et al.*'s method[30] and the molecular weights for γ-PAN fractions were indirectly evaluated from the MHS equation, established for R-PAN in a dimethyl sulfoxide (DMSO) solution, assuming that the MHS equation for good solvent is independent of the stereoregularity of the polymer.

Very recently, Kamide and his coworkers[32,33] succeeded in determining the pentad tacticity of R- and γ-PANs from ^{13}C NMR spectra in deuterated dimethyl sulfoxide (DMSO-d_6) and disclosed that R-PAN is polymerized according to Bernoulli statistics and γ-PAN obeys 1st-order Markov statistics.

R-PAN has therefore relatively low stereoregularity as compared with γ-PAN. The weight fraction of *mmmm* sequence (*m*; meso configuration) was estimated to be 0.07 for R-PAN and 0.37 for γ-PAN.

In this article, an attempt was made to investigate the dilute solution properties of γ-PAN whose stereoregularity is clarified in greater detail and compare the results obtained here with those of R-PAN.

EXPERIMENTAL

Polymer Samples

γ-PAN was polymerized according to the method of White.[34] Analytical reagent grade urea, manufactured by Kishida Chemicals Co., Osaka, was purified by recrystallization with a mixture of water and methanol (1 : 5 by weight) and dried in hot air. Inhibitors, added to commercially available acrylonitrile (AN)

(analytical reagent grade, manufactured by Kishida Chemicals Co.) were extracted completely with a 2 wt% aq sodium carbonate solution and washed with water. Purified AN was mixed with purified urea to give a 1 : 1 (by weight) mixture, stored in a methanol–dry ice mixture at −78°C for 6 days. The AN–urea canal complex, formed slowly during storage, was irradiated with γ-ray from cobalt 60 at −78°C at a dose rate of 3×10^5 R h^{-1} for 5 h (The irradiation dose was 1.5 MR.) The polymer was dissolved in DMSO and precipitated with methanol. The polymerization yield was 58 wt%. The viscosity-average molecular weight $\bar{M}_v$ of the polymer was determined using the MHS equation (in DMSO, Table V) to be 1.70×10^5. For comparison, the R-PAN fractions in the previous paper[35] were used for light scattering and solution viscosity measurements in DMSO.

NMR Measurements

^{13}C NMR measurement on γ-PAN was made on a FT-NMR JEOL FX-400 using deuterated DMSO-d_6 as solvent at 80°C. This γ-PAN polymer was found to have an isotactic triad of 52%, heterotactic triad of 33% and syndiotactic triad of 15%. The corresponding triads for R-PAN fractions were 26, 50, and 24%, respectively. The pentad tacticity was evaluated by a method previously proposed.[32,33]

Wide-Angle X-Ray Diffraction

Wide-angle X-ray diffraction for as-polymerized γ- and R-PAN whole polymer powders and the precipitated powder of γ-PAN from the solution was measured on a Rigaku RU 200 PL type X-ray diffraction apparatus.

Solvents

Reagent-grade DMSO, dimethylacetamide (DMAc), ethylene carbonate (EC), γ-butyrolactone, and 70 wt% aq nitric acid, supplied by Kishida Chemicals Co., Osaka, were used as received. The Concentration of nitric acid was adjusted by adding pure water. The R-PAN sample, prepared in the previous paper,[35] had a residue of the redox catalyst, $\sim SO_3H$, at the chain end and to suppress the ionization of the end group when dissolved in a solvent, 0.1 wt% LiCl was added to the solvents. Since γ-PAN was synthesized without any catalyst, no LiCl was necessary.

Solvation

The adiabatic compressibility of the solution was calculated from the sound velocity and density of the solution and converted to the weight of the solvated solvent per gram of polymer N_s using Passynsky's relation. The sound velocity was measured on a Nusonics Model 6080 Concentration Analyzer at 25 ± 0.005°C in the polymer concentration range of 1—5 g polymer/100 g solvent. The details of the measuring conditions have been described already.[35]

Fractionation

A whole γ-PAN sample was fractionated by a successive precipitation (SPF) method[36] using DMSO as a solvent and toluene as a non-solvent. The successive solution method, proved to be theoretically much more effective to obtain sharp fractions, could not be applied here due to extreme difficulty in diluting with DMSO a polymer-rich phase separated after two-phase equilibrium. SPF was conducted under the following conditions: concentration of starting solution, 2 g/100 ml; initial concentration, 0.95 g/100 ml for the first fraction; temperature 30°C; total number of fractions, 20.

Light Scattering

A Union Giken LS 601 type light scattering photometer was used at 25°C for measurements on DMSO solutions. The wave length λ_0 of the polarized He-Ne laser incident light was 633 nm. The experimental data were analyzed by Zimm's procedure to determine the weight-average molecular weight $\bar{M}_w$, the

radius of gyration $\langle S^2 \rangle_z^{1/2}$ and the second virial coefficient A_2.

A Fica photogoniodiffusiometer 42000 was employed also for aq nitric acid solutions at $\lambda_0 = 546$ nm. The details of the experiments and analytical procedure are described elsewhere[35] and $\langle S^2 \rangle_z^{1/2}$ and A_2 were evaluated.

The specific refractive index increment $d\tilde{n}/dC$ for γ-PAN was determined to be 0.038 ml g^{-1} by a Union Giken RM 102 type differential refractiometer at 25°C at $\lambda_0 = 633$ nm, which is in an excellent agreement with that for R-PAN (0.038 ml g^{-1}).

Solution Viscosity

Solution viscosity was measured in DMSO and 57 and 67 wt% aq nitric acids with a modified Ubbelohde suspension type viscometer at 25±0.01°C. $[\eta]$ was determined by Huggins plot.

RESULTS AND DISCUSSION

Table I shows the pentad tacticity data for three typical γ-PAN fractions and a whole R-PAN sample. in the table, the data for a whole R-PAN are cited from the previous paper.[33] The pentad tacticity of γ-PAN is almost independent of its average-molecular weight. The content of a *mmmm* sequence is about 4.8 times larger than that of R-PAN and the content of a *rmrm* sequence (*r*, racemo configuration) is only 0.6 times that of R-PAN. These facts indicate that γ-PAN has a higher stereoregularity than R-PAN.

By applying the pentad method[33] to the tacticity data, we evaluated the probability of linking a meso sequence to a racemo sequence, $P(m/r)$ and that of linking a racemo sequence to a meso sequence, $P(r/m)$ for each γ-PAN sample as listed in the bottom lines of Table I. The probability of a meso arrangement P_m, in Bernoulli statistics, for R-PAN was cited from a reference.[33]

With the aid of electric computer, we generated meso- and racemo sequences in PAN molecules with the degree of polymerization ($N = 4001$) by Monte Carlo method under the following conditions: $P(m/r) = 0.518$, $P(r/m) = 0.197$ for γ-PAN and $P_m = 0.519$ for R-PAN.

Table I. The observed pentad fractions for γ-PAN fractions and R-PAN

Pentad sequence	γ-PAN			R-PAN
	$\bar{M}_w \times 10^{-4}$			
	9.8	26.3	34.8	18.8[a]
mmmm	0.387	0.386	0.350	0.077
mmmr	0.125	0.112	0.108	0.125
rmmr	0.042	0.034	0.043	0.068
mmrm	0.117	0.120	0.118	0.125
mmrr	0.068	0.074	0.076	0.097
rmrm	0.083	0.082	0.096	0.149
rmrr	0.050	0.052	0.063	0.129
mrrm	0.029	0.028	0.030	0.055
mrrr	0.045	0.055	0.052	0.112
rrrr	0.054	0.056	0.062	0.065
			Average	
$P(r/m)$	0.191	0.189	0.210 (0.197)	
$P(m/r)$	0.536	0.509	0.508 (0.518)	

[a] Reference 33.

We define the number of "blocks" for *i*-th molecule, which consists of p of meso sequences, $m_1 \cdots m_p$, as $F_m^i(p)$ and the number of "blocks" for the same molecule, which consists of q of racemo sequences, $r_1 \cdots r_q$, as $F_r^i(q)$, respectively (see Figure 1). Then, $F_m^i(p)$ and $F_r^i(q)$ for *i*-th molecule can be averaged over all chains ($i = 1 \sim I$) comprising the sample and denoted by $\overline{F_m(p)}$ and $\overline{F_r(q)}$, respectively. $\overline{F_m(p)}$ and $\overline{F_r(q)}$ are given by

$$\left.\begin{aligned} \overline{F_m(p)} &= \frac{\sum_{i=1}^{I} F_m^i(p)}{I} \\ \overline{F_r(q)} &= \frac{\sum_{i=1}^{I} F_r^i(q)}{I} \end{aligned}\right\} \quad (2)$$

When I is sufficiently large, equation 2 reduces to equation 2′

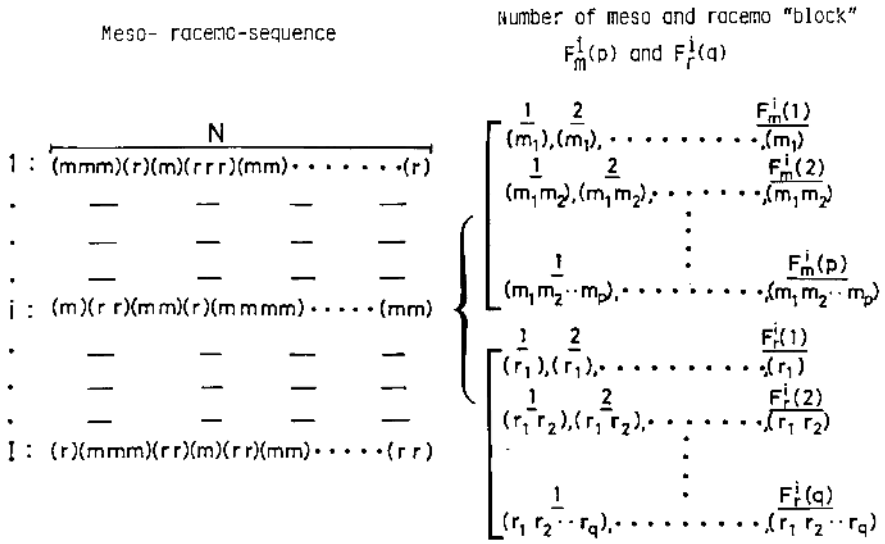

Figure 1. Meso- and racemo-sequence distribution of polyacrylonitrile and the number of "blocks" $F_m^i(p)$ or $F_r^i(p)$.

Table II. Distribution of meso- and racemo-sequence of γ-PAN and R-PAN ($M=21.2\times10^4$)

Polymer	p or q	1	2	3	4	5	6	7	8	9	10	11	12	13	14	15	16	17	18	19	20	21	22	23	24	25
γ-PAN	$\overline{F_m(p)}$	114	92	73	59	47	38	30	24	20	16	13	10	8	7	5	4	3	3	2	2	1	1	1	1	1
	$\overline{F_r(q)}$	301	143	68	33	16	7	4	2	1	1	0	0	0	0	0	0	0	0	0	0	0	0	0	0	0
R-PAN	$\overline{F_m(p)}$	480	249	129	67	35	18	9	5	3	2	1	1	0	0	0	0	0	0	0	0	0	0	0	0	0
	$\overline{F_r(q)}$	517	249	120	58	28	13	6	3	2	1	1	0	0	0	0	0	0	0	0	0	0	0	0	0	0

$$\left.\begin{aligned}\overline{F_m(p)} &= B_m P_A P_B^{p-1}\\ \overline{F_r(q)} &= B_r P_C P_D^{q-1}\end{aligned}\right\} \qquad (2')$$

Here, B_m (or B_r) is the total number of meso- (or racemo-) sequence blocks in the molecule, and expressed as,

$$\left.\begin{aligned}B_m &= \sum_{i=1}^{I}\sum_{p=1}^{N-1} F_m^i(p)/I\\ B_r &= \sum_{i=1}^{I}\sum_{q=1}^{N-1} F_r^i(q)/I\end{aligned}\right\} \qquad (3)$$

$P_A=P(r/m)$, $P_B=1-P(r/m)$, $P_C=P(m/r)$, and $P_D=1-P(m/r)$ for γ-PAN and $P_A=1-P_m$, $P_B=P_m$, $P_C=P_m$, and $P_D=1-P_m$ for R-PAN.

$\overline{F_m(p)}$ and $\overline{F_r(q)}$ for all possible p or q for γ- and R-PAN were calculated using eq 2′ and 3 from $P(r/m)$ and $P(m/r)$ and P_m values in Table I and putting $I=100$ and $N=4001$ (*i.e.*, molecular weight $M=2.12\times10^5$). The results are summarized in Table II. The details of calculation will be published elsewhere.[37] Of course, $F_m^i(p)$ and $F_r^i(q)$ have some distributions around $\overline{F_m(p)}$ and $\overline{F_r(q)}$, respectively.

We chose six solvents among good solvents, widely used hitherto, for R-PAN to examine solvent power against γ-PAN. For this purpose, four grams of the whole polymer sample ($\bar{M}_v=1.70\times10^5$) were mixed with 100 ml of solvent at 60°C for 5 h. As-polymerized γ-PAN dissolved completely

after mixing in both DMSO and 67 wt% aq nitric acid, but only 0.2 wt% solutions were obtained in DMF, DMAc, EC, and γ-butyrolactone. In the latter group of solvents, the undissolved polymer did not even swell. When powder-like γ-PAN, precipitated with methanol from 4 g/100 ml solution of as-polymerized polymer in DMSO, was mixed again at 60°C with DMAc, the solubility of the polymer increased remarkably up to 3.62 wt%. The stereoregularity of the dissolved and undissolved parts of γ-PAN precipitate/DMAc mixture, isolated by centrifuging under 4.9×10^4 G for 1 h, was estimated by ^{13}C NMR method in DMSO-d_6. It was confirmed that there was only slight a difference in the stereoregularity between two parts: isotactic triad, 48.6%, heterotactic triad, 37.3%, and syndiotactic triad, 14.1% for the soluble part, and 53.3, 33.6, and 13.1 % for the insoluble part.

Figure 2 shows X-ray diffraction patterns of as-polymerized and precipitated powders from DMSO solution of unfractionated γ-PAN and R-PAN samples. As-polymerized γ-PAN has a higher crystallinity and larger crystalline size than precipitated γ-PAN and as-polymerized R-PAN. This strongly suggests that the crystallinity, besides the stereoregularity, governs mainly the solubility of PAN in solvents.

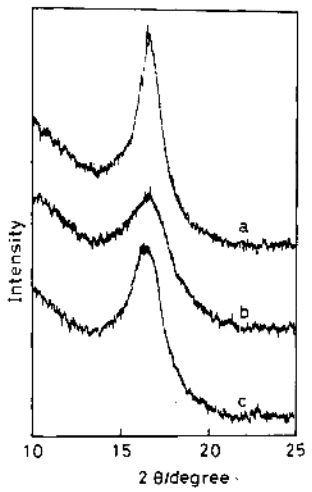

Figure 2. X-Ray diffraction patterns: a) as-polymcrized γ-PAN; b) precipitated powder of γ-PAN from DMSO solution; c) as-polymerized R-PAN.

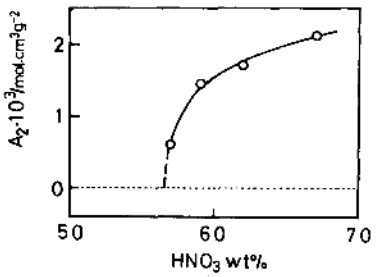

Figure 3. Variation in the second virial coefficient A_2 of a γ-PAN fraction (γ-1-3) with nitric acid concentration.

Figure 3 shows A_2, as determined by the light scattering method, of solutions of a γ-PAN fraction (Sample cord γ-1-3) dissolved in 57, 59, 62 and 67 wt% aq nitric acid at 25°C. The sample had $\bar{M}_w$ of 1.68×10^5, determined by the light scattering method in DMSO. The nitric acid concentration of a solvent, in which A_2 becomes zero at 25°C, can be extrapolated from Figure 3 to be 56.5 wt%. That is, 56.5 wt% aq nitric acid can be regarded as a Flory's theta solvent of γ-PAN at 25°C. Kamide *et al.* determined the Flory's theta solvent of R-PAN to be 55 wt% aq nitric acid at 25°C.[35] Then, theta solvent for γ-PAN is slightly higher in nitric acid concentration than that for R-PAN. The light scattering measurement on γ-PAN in 56.5 wt% aq nitric acid was attempted, but was unsuccessful due to experimental difficulty in exclusion of gel-like materials during filtration.

Table III shows $\bar{M}_w$, $\langle S^2 \rangle_z^{1/2}$, A_2 and $[\eta]$ of eight γ-PAN fractions in DMSO, 67 and 57 wt% aq nitric acids. Table IV summarizes similar data for R-PAN in DMSO at 25°C. In the table, $\bar{M}_w$ data in DMF in the previous paper[35] are tabulated for comparison. Table IV indicates that $\bar{M}_w$ values obtained for R-PAN in DMSO are in good agreement with those in DMF within an experimental un-

Table III. Results of light scattering and limiting viscosity number for γ-PAN fractions in various solvents at 25°C

Sample	$\bar{M}_w \times 10^{-4}$	$\langle S^2 \rangle_z^{1/2} \times 10^8$/cm			$A_2 \times 10^3$ [a]	$[\eta]$/cm^3 g^{-1}		
	DMSO	DMSO	67 wt%HNO_3	57 wt%HNO_3	DMSO	DMSO	67 wt%HNO_3	57 wt%HNO_3
γ-1-1	7.1	152	145	143	0.79	135	130	100
γ-1-2	10.7	193	189	176	0.83	166	168	125
γ-1-3	16.8	242	243	220	0.59	224	216	161
γ-1-4	26.3	317	312	275	0.60	275	272	182
γ-1-5	34.8	348	359	317	0.53	347	329	222
γ-1-6	51.2	443	—	—	0.40	408	396	—
γ-1-7	61.5	507	489	432	0.50	473	460	300
γ-1-8	78.3	544	565	487	0.47	540	520	342

[a] cm^3 mol g^{-2}.

Table IV. Results of light scattering and limiting viscosity number for R-PAN fractions in DMF and DMSO at 25°C

Sample	$\bar{M}_w \times 10^{-4}$		$\langle S^2 \rangle_z^{1/2} \times 10^{8}$ [b]	$A_2 \times 10^{3}$ [c]	$[\eta]$ [d]
	DMF[a]	DMSO	DMSO	DMSO	DMSO
PAN-1	5.2	—	—	—	100
PAN-2	7.5	—	—	—	124
PAN-3	10.7	10.0	185	1.60	146
PAN-4	15.8	—	—	—	190
PAN-5	21.5	22.0	269	1.15	226
PAN-6	31.2	33.3	329	0.70	278
PAN-7	52.0	50.8	438	0.82	400

[a] Reference 35. [b] cm. [c] cm^3 mol g^{-2}. [d] cm^3 g^{-1}.

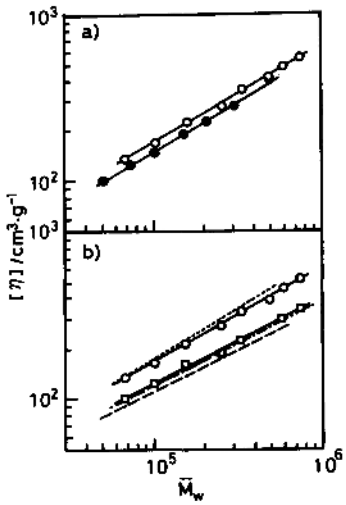

Figure 4. Log–log plots of the limiting viscosity number $[\eta]$ *versus* the weight-average molecular weight $\bar{M}_w$ for γ-PAN and R-PAN. a) ○, γ-PAN in DMSO; ●, R-PAN in DMSO. b) ○, γ-PAN in 67 wt% aq HNO_3; □, γ-PAN in 57 wt% aq HNO_3; dot-dash line, γ-PAN in 56.5 wt% aq HNO_3; dotted line, R-PAN in 67 wt% aq HNO_3; broken line R-PAN in 55 wt% aq HNO_3.

certainty (±7%) and R-PAN molecule dissolves molecularly in DMSO and DMF.

Figure 4 shows the log-log plot of $[\eta]$ against $\bar{M}_w$ of γ-PAN and R-PAN in DMSO and aq nitric acids. Here, the data of R-PAN in aq nitric acid are cited from the previous paper.[35] MHS equations were evaluated using the least-squares method and the results are summarized, together with those for R-PAN in various solvents in literature,[35] in Table V. In DMSO solutions, $[\eta]$ for γ-PAN is significantly larger than that for R-PAN if the samples with the same $\bar{M}_w$ are compared. In contrast to this, in 67 wt% aq nitric acid $[\eta]$ of R-PAN is just slightly larger than that of γ-PAN if $\bar{M}_w > 2 \times 10^4$, but the difference is insignificant. The effect of stereospecificity becomes significant with the MHS equation in DMSO, but not in aq nitric acid.

$[\eta]$ of a γ-PAN solution in 57 wt% aq nitric acid ($a = 0.503$), is in the vicinity of the theta solvent and about 15% larger than that of R-PAN in 55 wt% aq nitric acid, in which

$A_2=0$, if the same $\bar{M}_w$ are compared.

Using the experimental relation between $[\eta]$ and the concentration of nitric acid, the $[\eta]$ value in a 56.5 wt% nitric acid was extrapolated and the following MHS relation was obtained:

$$[\eta]=0.365\ \bar{M}_w^{0.50_1}\ (\mathrm{cm^3\,g^{-1}}) \qquad \text{(a)}$$

The exponent in eq a coincides well with 0.5, as anticipated if 56.5 wt % aq nitric acid is a theta solvent. Equation a is shown as a dot-dash line in Figure 4b. In theta solvents, $[\eta]$ of γ-PAN is some 8.5% larger than that of R-PAN, if the samples have the same $\bar{M}_w$. In a good solvent, such as 67 wt% aq nitric acid, MHS equations are not significantly influenced by the stereoregularity of PAN, but in a poor solvent, the situation is different.

Kamide and Terakawa[28] observed that γ-PAN dissolves in ethylene carbonate at 60°C, in which the exponent a in MHS equation equals with 0.5:

$$[\eta]=0.295\ \bar{M}_v^{0.50}\ (\mathrm{cm^3\,g^{-1}}) \qquad \text{(a')}$$

Here, $\bar{M}_v$ in eq a' was evaluated using MHS eq obtained by Kamide and Terakawa[28] for R-PAN in DMSO, assuming that the above equation is valid independent of stereoregularity. The polymer prepared in this study dissolved only partially in EC and the polymer–solvent mixture became obviously turbid and any solution viscosity measurements were impossible. Then, some significant differences in the stereospecificity and/or the crystallinity should be considered between two γ-PAN polymers synthesized in Kamide–Terakawa's[28] and the present work.

Figure 5 shows the log–log plot of $\langle S^2\rangle_z^{1/2}$ and $\bar{M}_w$ of the γ-PAN and R-PAN in DMSO and in aq nitric acids. The semi-empirical relation between $\langle S^2\rangle_z^{1/2}$ and $\bar{M}_w$ is in the form,

$$\langle S^2\rangle_z^{1/2}=K_\gamma \bar{M}_w^{\gamma} \qquad (4)$$

and was determined by the least-squares method and the parameters K_γ and γ evaluated thus are compiled in the fifth and sixth columns of Table V. $\langle S^2\rangle_z^{1/2}$ of γ-PAN is larger than that of R-PAN, when both polymers with constant $\bar{M}_w$ are dissolved in DMSO, but the former is very slightly smaller in a 67 wt% aq nitric acid than the latter. Same tendency was also observed in MHS relations of these polymer solutions. Using the dependence of

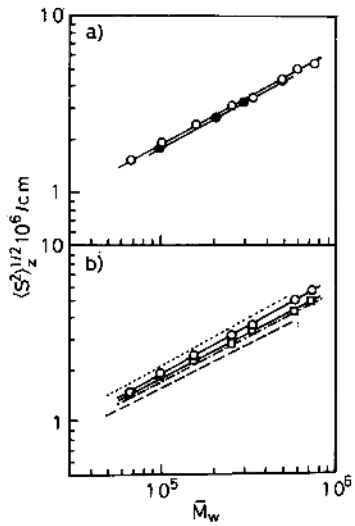

Figure 5. Plots of the radius of gyration $\langle S^2\rangle_z^{1/2}$ as a function of the weight-average molecular weight $\bar{M}_w$ for γ-PAN and R-PAN. Marks have the same meaning as those in Figure 4.

Table V. K_m and a in Mark–Houwink–Sakurada equations and K_γ and γ in relations between $\langle S^2\rangle_z^{1/2}$ and $\bar{M}_w$ for γ-PAN and R-PAN in various solvents at 25°C

Polymer	Solvent	K_m	a	$K_\gamma\times 10^8$	γ
γ-PAN	DMSO	0.204	0.58_0	0.378	0.54
	67 wt%HNO_3	0.217	0.57_3	0.320	0.55
	57 wt%HNO_3	0.363	0.50_3	0.472	0.51
	56.5 wt%HNO_3	0.365	0.50_1	0.474	0.51
R-PAN	DMSO	0.153	0.60_0	0.337	0.54
	67 wt%HNO_3[a]	0.122	0.62_2	0.359	0.55
	55 wt%HNO_3[a]	0.342	0.50_1	0.480	0.50
	DMF[a]	0.052	0.69_0	0.317	0.55
	85 wt%EC[a]	0.256	0.49	0.431	0.50

[a] Reference 35.

$\langle S^2\rangle_z^{1/2}$ on the concentration of nitric acid, as illustrated in Figure 6, we estimated $\langle S^2\rangle_z^{1/2}$ value of γ-PAN in 56.5 wt% aq nitric acid (that is, $\langle S^2\rangle_{o,z}^{1/2}$, the suffix o denotes the unperturbed state) and obtained

$$\langle S^2\rangle_{o,z}^{1/2} = 0.474 \times 10^{-8} \bar{M}_w^{0.51} \text{ (cm)} \quad \text{(b)}$$

The relation (b) is shown in Figure 5b as a dot-dash line. In theta solvents, $\langle S^2\rangle_z^{1/2}$ of γ-PAN is larger than that of R-PAN if the same $\bar{M}_w$ are compared. In other words, the effect of the stereoregularity on $\langle S^2\rangle_z^{1/2}$ *vs.* $\bar{M}_w$ relations is significant in a theta solvent.

Figure 7 shows the Flory's viscosity parameter Φ ($\equiv[\eta]\bar{M}_w\ q_{w,z}/6^{3/2}\langle S^2\rangle_z^{3/2}$, $q_{w,z}$, correction factor for polydispersity, was calculated assuming the Schulz–Zimm distribution and the ratio of weight- to number-average molecular weight $\bar{M}_w/\bar{M}_n(=1.3)$[35] for γ-PAN and R-PAN plotted as a function of $\bar{M}_w$ for the solutions of γ-PAN in DMSO, 67 wt% aq nitric acid and 57 wt% aq nitric acid and the R-PAN in DMSO. Φ values remain nearly constant, giving an averaged value of $(2.6\pm 0.3)\times 10^{23}$. There is no significant difference in Φ between γ- and R-PAN.

Figure 8 shows the plot of A_2 as a function of $\bar{M}_w$ for γ-PAN and R-PAN in DMSO at 25°C. As expected A_2 for γ-PAN is smaller than that for R-PAN.

The unperturbed chain dimension A ($\equiv(\langle R^2\rangle_o/M)^{1/2}$, $\langle R^2\rangle_o^{1/2}$, the mean-square end-to-end distance of the unperturbed chain) was determined by using the following methods:

Method 2A

$\langle S^2\rangle_z^{1/2}$ of a polymer in a Flory theta solvent (in this case, 56.5 wt% aq nitric acid at 25°C) allows A to be determined from

$$A = 6^{1/2}(\langle S^2\rangle_o/M)^{1/2} \quad (5)$$

Method 2B

$$A = 6^{1/2}(\langle S^2\rangle_o/M)^{1/2} = 6^{1/2}(\langle S^2\rangle/M\alpha_s^2)^{1/2} \quad (6)$$

α_s is the linear expansion factor, calculated using the penetration function ψ from A_2, $\bar{M}_w$, and $\langle S^2\rangle_z^{1/2}$ data. Here, Kurata–Fukatsu–Sotobayashi–Yamakawa theory,[38] connecting ψ with the excluded volume parameter z and the Fixman theory[39] of the excluded volume effect are utilized.

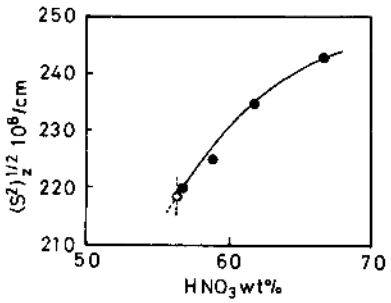

Figure 6. Variation in the radius of gyration $\langle S^2\rangle_z^{1/2}$ with nitric acid concentration for a γ-PAN fraction (γ-1-3). ●, experimental data; ○, extrapolated point to a theta solvent.

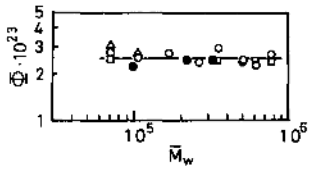

Figure 7. Molecular weight dependence of Flory's viscosity parameter Φ. ○, γ-PAN in DMSO; □, γ-PAN in 57 wt% aq. HNO_3; △, γ-PAN in 67 wt% aq HNO_3; ●, R-PAN in DMSO.

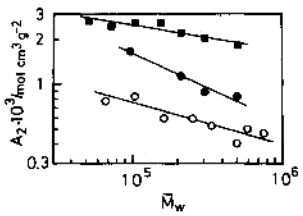

Figure 8. Molecular weight dependence of the second virial coefficient A_2 for γ-PAN in DMSO (○), R-PAN in DMSO (●), and R-PAN in DMF (■).

Method 2C (Baumann plot)[40]

$$(\langle S^2\rangle/M)^{3/2} = A^3/6^{3/2} + 1/(4\pi^{3/2})BM^{1/2} \quad (7)$$

where B is the long-range interaction parameter.

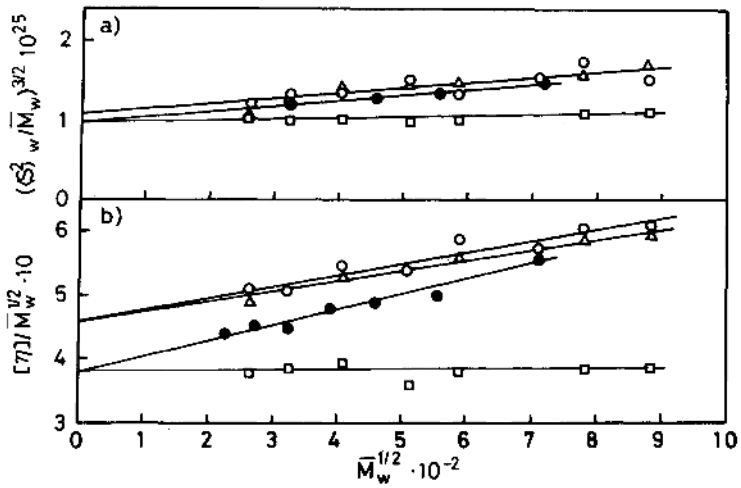

Figure 9. a) Baumann plot (method 2C), b) Stockmayer–Fixman Plot (method 2E): ○, γ-PAN in DMSO; △, γ-PAN in 67 wt% aq HNO_3; □, γ-PAN in 57 wt% aq HNO_3; ●, R-PAN in DMSO.

Table VI. Unperturbed chain dimension A, long-range interaction parameter B, conformation parameter σ and characteristic ratio C_∞ of γ-PAN and R-PAN in various solvents at 25°C

Polymer	Solvent	$A\times10^8$/cm						σ	C_∞	$B\times10^{27}$/cm^3	
		2A	2B	2C	2E	2F	Most probable			2C	2E
γ-PAN	DMSO	-	1.19	1.17	1.17	1.20	1.18	2.80	15.5	1.18	0.94
	67 wt%HNO_3			1.17	1.17	1.20	1.18	2.80	15.5	1.18	0.91
	57 wt%HNO_3	—	—	1.12	1.10	1.09	1.10	2.61	13.5	0.09	0.01
	56.5 wt%HNO_3	1.13	—	1.12	1.08	1.08	1.10	2.61	13.5	0	0
R-PAN	DMSO	—	—	1.12	1.09	1.10	1.10	2.61	13.5	1.51	1.19
	67 wt%HNO_3[a]	—	—	1.29	1.29	1.30	1.29	3.06	18.5	3.17	2.69
	55 wt%HNO_3[a]	1.06	—	1.06	1.06	1.06	1.06	2.51	12.6	0	0
	DMF[a]	—	—	1.09	1.05	1.05	1.06	2.51	12.6	2.33	2.32
	85 wt%EC[a]	0.95	—	0.95	0.96	0.96	0.95	2.25	10.1	0	0

[a] Reference 35.

Method 2E (Stockmayer–Fixman plot)[41]

$$[\eta]/M^{1/2}=K+2(3/2\pi)^{3/2}\Phi_0(\infty)BM^{1/2} \quad (8)$$

with

$$K=\Phi_0(\infty)A^3 \quad (9)$$

and

$$\Phi_0(\infty)=2.87\times10^{23} \quad (10)$$

Method 2F (Kamide–Moore plot)[42]

$$-\log K_m+\log[1+2\{(a-0.5)^{-1}-2\}^{-1}] = -\log K+(a-0.5)\log M_0 \quad (11)$$

where M_0 can be approximated with a geometrical average of the upper and lower limits of molecular weights, in which MHS eq is applicable.

Figure 9a and b show Baumann (Method

2C) and Stockmayer–Fixman (Method 2E) plots of γ-PAN (open mark) and R-PAN (closed mark) fractions. The intercept and slope of these plots enable us to estimate A and B, respectively.

Table VI summarizes A and B values estimated thus and A values evaluated by methods 2B and 2F. Then, we can regard as an average of the A values estimated by methods 2A, 2B, 2C, 2E, and 2F as the most probable value shown in the 8th column of the table. The table contains also the A values of R-PAN in 67 and 55 wt% aq nitric acid, DMF and 85 wt% EC for comparison.[35]

In DMSO, A(γ-PAN) > A(R-PAN) and B(γ-PAN) < B(R-PAN) hold and in consequence, [η](γ-PAN) > [η](R-PAN). In 67 wt% aq nitric acid, A(γ-PAN) is unexpectedly 9% smaller than A(R-PAN). In other solvents, A(γ-PAN) is always larger than A(R-PAN). In DMSO γ-PAN has an A value 7% larger than R-PAN, but in 67 wt% aq nitric acid the reverse is true. Extrapolated A value of γ-PAN in 56.5 wt% aq nitric acid (theta solvent) is 4% larger than the experimentally directly measured value of A for R-PAN in 55 wt% aq nitric acid (theta solvent). The effect of microtacticity on A of PAN is more remarkable in 67 wt% aq nitric acid than in DMSO.

For example, $\langle S^2 \rangle_{o,z}^{1/2}$ for sample cord γ-1-3($\bar{M}_w = 16.8 \times 10^4$) in theta solvent (*i.e.*, 56.5 wt% aq nitric acid) was estimated to be 218×10^{-8} cm (see, Figure 6), and accordingly, A was found to be 1.13×10^{-8} cm. This value is in good agreement with that estimated for γ-PAN in 56.5 wt% aq nitric acid by method 2C. A values are practically constant in 56 ~ 57 wt% aq nitric acid.

The ratio of B of R-PAN to γ-PAN in 67 wt% aq nitric acid is 2.96 and the similar ratio in DMSO is only 1.28. In other words, 67 wt% aq nitric acid is a very good solvent for R-PAN, but is not a very good solvent for γ-PAN at the same temperature. A and B values of γ-PAN in DMSO are the same as those in 67 wt% aq nitric acid, respectively, and accordingly, MHS equations are almost same in the two solvents. For the poor solubility of γ-PAN, as described before, not only the higher crystallinity, but also low B values are responsible phenomenologically.

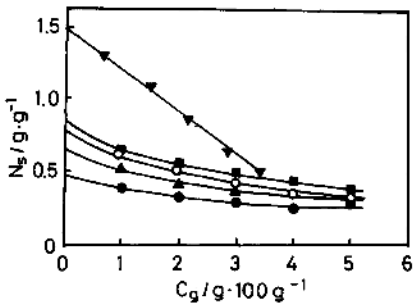

Figure 10 Plots of N_s *versus* concentration C_g at 25°C, for γ-PAN in DMSO (○), R-PAN in DMSO (●), in DMAc (▲), in DMF (■), and 67 wt% aq HNO_3 (▲).

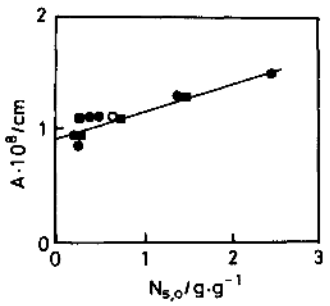

Figure 11 $N_{s,o}$ dependence of the short-range interaction parameter A for γ-PAN (○), R-PAN (●) and the acrylonitrile–methyl acrylate copolymer (■).[32]

Figure 10 shows the dependence of the weight of solvated solvent per gram of polymer N_s on the polymer concentration C_g (g/100 g solution) for γ-PAN (open mark) and R-PAN (closed mark) in various organic solvents. N_s decreases very gradually with an increase in C_g and there is no significant difference in N_s or $N_{s,o}$ of ($\equiv \lim_{c_g \to 0} N_s$) between γ-PAN and R-PAN. Figure 11 shows the dependence of A on $N_{s,o}$ of PANs in various solvents. A of γ-PAN is located just on a common plot for R-PAN and the AN/MA copolymer, obtained in the previous paper.[35] The solvation is not remarkable even for

γ-PAN solution and the larger difference in solubility behavior of these two PAN polymers in organic solvents cannot be interpreted by the solvation concept.

In order to confirm the above conclusions, we investigated the chemical shifts of CH carbon and CN carbon of γ-PAN and R-PAN in DMSO-d_6. Peaks of CH and CN carbons of γ-PAN were located at almost the same magnetic field, suggesting that a specific interaction between some functional groups in PAN and the solvent does not depend on the stereospecificity of PAN.

γ-PAN and R-PAN molecules consist of the same monomer units, but are notably different in steric configurations (Table I). Then, the significant difference in the long-range interaction, expressed by B parameter, between γ-PAN and R-PAN, cannot be explained if the interaction only occurs between the monomer unit and solvent molecule. We can suppose that the some sequence of monomer units interacts with the solvent molecule and the sequence distribution differences between two polymer types as demonstrated in Table II bring about the large differences in B parameters, especially in 67 wt% aq nitric acid. On the 9th and 10th columns of Table VI collects, the steric factor σ, is defined as

$$\sigma = A/A_f \tag{12}$$

(where A_f is A of a hypothetical chain with free internal rotation (model I) and $A_f = 0.423 \times 10^{-8}$ cm for PAN) and the characteristic ratio C_∞ is given by

$$C_\infty = A^2 M_b / l^2 \tag{13}$$

(where M_b is the mean molecular weight per skeletal bond (=26.5) and l is the mean bond length (1.54×10^{-8} cm), both calculated from the most probable A value).

Figure 12 shows the effect of the side chain molecular weight on σ of the vinyl-type polymers. All the data except for γ-PAN are cited from the literature.[35,43] The closed circle is an average value and the full line denotes the range of variation of σ. Except PAN, σ is roughly in linear proportion to the molecular weight of the side chain group, as expressed by a broken line in the figure. R- and γ-PAN data are located on points much higher than the broken line, indicating that introduction of a CN group to a vinyl monomer brings about unexpectedly large stiffness in the polymer chain. This stiffness cannot be interpreted by a simple steric hindrance due to the molar volume of the side chain. Dondos and Benoit[44] showed that dependence of σ of the polymer with non-polar side groups, such as PE, PP, and PS on the molar volume of the side group can be approximately represented by a straight line and σ of the polymer with polar side groups like nitrile or alcohol is larger than that of non-polar polymer.

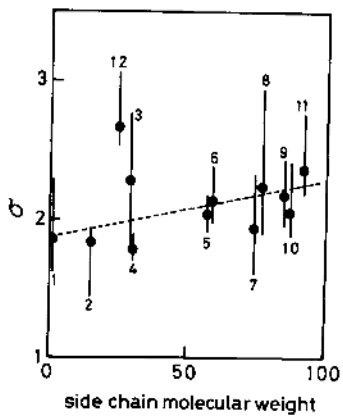

Figure 12. Effect of the molecular weight of the side chain on the conformation parameter σ for vinyl-type polymers:[43] 1, polyethylene; 2, polypropyrene; 3, poly(1-butene); 4, polyisobutene; 5, poly(1-pentene); 6, poly(vinyl acetate); 7, poly(methyl methacrylate); 8, polystyrene; 9, poly(1-octaine), 10, polyisopropyl acrylate; 11, poly(α-methylstyrene); 12, polyacrylonitrile.

Very recently, Kamide *et al.*[32] observed from the ^{13}C NMR spectra of γ-PAN and R-PAN in DMSO-d_6 that the intensity ratio of three triad peaks of CH carbon is just the reverse of that of CN carbon from a higher magnetic field and then the isotactic triad peak was concluded to shift to a higher mag-

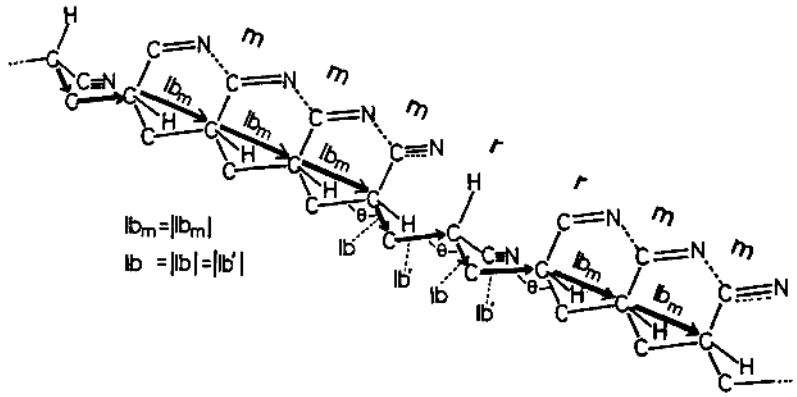

Figure 13. Polyacrylonitrile chain model.

netic field, suggesting isotactic CH carbon to be strongly shielded as compared with syndiotactic and heterotactic triad CH carbons. If the CN group is free and triple bond exists between C and N, such a strong shield effect cannot be expected. In other words, the shielding effect is caused only in the case when CN groups have a double bond nature, and the meso part of PAN may have a *trans–trans* or almost *trans–trans* conformation. The former conformation might stiffen the meso sequence in the solution. Additional experimental facts supporting this idea are (1) the lower magnetic field component of CN carbon peaks becomes sharp and (2) there is a specific interaction of Cu^{2+} ion with CN group in the meso sequence.[45]

If the above-mentioned conclusion is acceptable, it is expected that γ-PAN is inflexible as compared with R-PAN. We can consider a hypothetical PAN chain, in which the meso sequence can be regarded as, at least partly, a rigid rod and the racemo sequence is freely rotatable. This chain is an alternative, extreme model (model II) for a hypothetical chain. Here, we assume that "blocks" consisting of less than n meso sequences ($m_1m_1m_2$, $m_1m_2m_3, \cdots$, $m_1 \cdots m_n$) are totally rigid rod and "blocks" consisting of a larger number of meso sequences than n can be divided into two or more rods with free rotation, whose number of meso sequences does not exceed

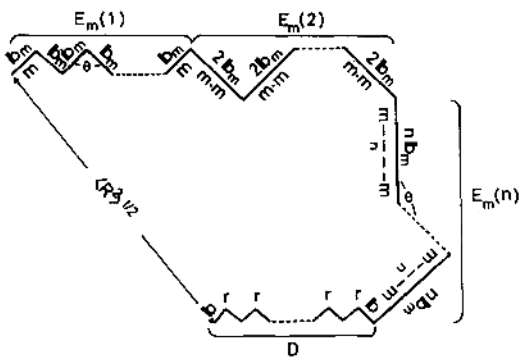

Figure 14. $\langle R^2 \rangle^{1/2}$ of model chain II.

n (see, Figures 13 and 14).

Here, we used the data in Table II for calculation of A_f of model II. For model II chain $A_{f,II}$ is given by

$$A_{f,II} = \langle R^2 \rangle_{f,II}^{1/2} / M^{1/2} \tag{14}$$

Consider a polymer chain consisting of L segments and represent vector of a segment constituting a polymer chain with $\boldsymbol{u}_i$ ($i = 1, \cdots, L$). The end-to-end distance vector $\boldsymbol{R}$ of the chain is

$$\boldsymbol{R} = \sum_{i=1}^{L} \boldsymbol{u}_i \tag{15}$$

and the mean-square end-to-end distance $\langle R^2 \rangle$ is given by

$$\langle R^2\rangle = \sum_{i=1}^{L} l_i^2 + 2\sum_{i=1}^{L}\sum_{\substack{j=1\\(i<j)}}^{L} l_i l_j (-\cos\theta)^{j-i} \quad (16)$$

if the chain permits a free internal rotation. Here, $l_i = |\boldsymbol{u}_i|$, $l_j = |\boldsymbol{u}_j|$ and θ is the bond angle.

In Figure 14, $\langle R^2\rangle_{\mathrm{of,II}}$ in equation 17 is given by (see Appendix)

$$\begin{aligned}\langle R^2\rangle_{\mathrm{f,II}} = {} & \sum_{x=1}^{n} E_m(x)(xb_m)^2 + Db^2 \\ & + 2\sum_{x=1}^{n}\left[\sum_{\substack{i=1\\(i<j)}}^{E_m(x)}\sum_{j=1}^{E_m(x)} (xb_m)^2(-\cos\theta)^{j-i}\right] \\ & + 2\sum_{\substack{i=1\\(i<j)}}^{D}\sum_{j=1}^{D} b^2(-\cos\theta)^{j-i} \\ & + 2\sum_{\substack{x=1\\(x<y)}}^{n}\sum_{y=1}^{n}\left[\sum_{\substack{i=1\\(i<j)}}^{E_m(x)}\sum_{j=1}^{E_m(y)} (xb_m)(yb_m) \right. \\ & \left. \times (-\cos\theta)^{\left(j-i+\sum_{h=x}^{y-1} E_m(h)\right)}\right] \\ & + \sum_{x=1}^{n}\left[\sum_{\substack{i=1\\(i<j)}}^{E_m(x)}\sum_{j=1}^{D} b(xb_m) \right. \\ & \left. \times (-\cos\theta)^{\left(j-i+\sum_{h=x}^{n} E_m(h)\right)}\right] \end{aligned} \quad (17)$$

Where

$$D = \sum_{q=1}^{q'} (2q\overline{F_r(q)})$$

(total number of b bond vector) (18)

and

$$E_m(h) = \sum_{k=0}^{k'} \overline{F_m(kn+h)} \quad (\text{for } h=1, \cdots, g') \quad (19a)$$

$$= \sum_{k=0}^{k'} \overline{F_m(kn+h)} - \overline{F_m(p')} \quad (\text{for } h=g'+1, \cdots, n-1) \quad (19b)$$

$$E_m(n) = \sum_{k=0}^{k'}\sum_{h=0}^{n-1} k\overline{F_m(kn+h)} - \sum_{h=g'+1}^{n-1} k'\overline{F_m(k'n+h)} \quad (19c)$$

b_m is the magnitude of vector $\boldsymbol{b}_m$ connecting two neighboring CN carbons in a meso sequence (Figure 13) ($\boldsymbol{b}_m = |\boldsymbol{b}_m|$), b is the magnitude of bond vector $\boldsymbol{b}$ in a main chain ($b = |\boldsymbol{b}|$), θ is the bond angle, q' is the largest number of q existing in a chain. In deriving eq 17, we assumed (i) meso sequence $m_1m_2\cdots m_p$ can be divided into k rigid rod blocks, each consisting of meso sequence $m_1m_2\cdots m_n$, and a rigid rod block $m_1m_2\cdots m_g$;

$$p = kn+g (k=1, \cdots, k';\ g=0, \cdots, n-1) \quad (20)$$

we define g' ($\equiv p'-k'n$) as g for maximum p (p') in a chain, (ii) a block $m_1m_2\cdots m_x$ ($x \leqq n$) can be expressed by single bond vector $x\boldsymbol{b}_m$, (iii) a racemo configuration can be represented by two bond vectors $\boldsymbol{b}$ and $\boldsymbol{b}'$ (Figure 13) with the same magnitude b ($|\boldsymbol{b}| = |\boldsymbol{b}'| = b$), (iv) each bond angle between two arbitrarily chosen bond vector is the same, (v) the chain is an absolutely free rotating chain. D and $E_m(h)$, given in eq 18 and 19, give the total number of $\boldsymbol{b}$ vectors and h $\boldsymbol{b}_m$ vectors.

In eq 17, the first, second, third and fourth terms of the right-hand side are the scalar products of the meso bond vector ($x\boldsymbol{b}_m$), racemo bond vector $\boldsymbol{b}$, bond vector of a rigid meso block $m_1m_2\cdots m_x$($x\boldsymbol{b}_m$), and bond vector $\boldsymbol{b}$, respectively. The fifth term is the scalar product between two rigid meso blocks with different x and the last term is the scalar product between $\boldsymbol{b}_m$ and $\boldsymbol{b}$. Here, $b_m = 2.516$Å, $b = 1.54$ Å, and $\theta = 109.5$ were employed.

First, D, $E_m(h)$ and $E_m(n)$ were calculated by putting the values of $\overline{F_m(p)}$ and $\overline{F_r(q)}$ in Table II into eq 18, 19a, b, and c. Using the values of D, $E_m(h)$ and $E_m(n)$, thus calculated, $\langle R^2\rangle_{\mathrm{f,II}}$ was calculated from eq 17, $A_{\mathrm{f,II}}$ and σ were readily estimated from 14 and 12, respectively. The following quantities were, for example,

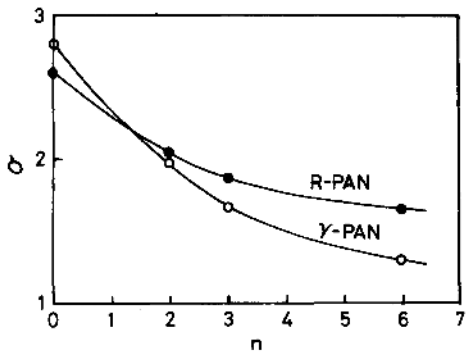

Figure 15. Plot of the conformation parameter σ as a function of the length of rigid rod meso-blocks n.

obtained: For γ-PAN, $D=2818$, $E_m(1)=318$, $E_m(2)=1273$; for R-PAN, $D=3860$, $E_m(1)=657$, $E_m(2)=716$ at $n=2$.

Figure 15 shows σ ($\equiv A/A_{f,n}$) as a function of n for γ- and R-PAN. Evidently, σ for both polymers decreases monotonously with an increase in n (*i.e.*, the rigidity of a meso sequence). When no additional effect, besides the steric hindrance due to the molar volume of the side group, exists, σ for PAN is roughly estimated from Figure 12 to be 2. Reversely, we can evaluate n to be ~ 2 for γ- and R-PAN from $\sigma \cong 2$.

Summarizing (1) γ-PAN does not have the same MHS equations as R-PAN, even in 67 wt% aq nitric acid and DMSO. In these solvents, the exponent a is not larger than 0.6. In this sense, there is no true good solvent for γ-PAN. (2) For R-PAN, it is expected that DMF is a better solvent than DMSO. But γ-PAN does not dissolve, at least, at room temperature in DMF. (3) A 56.5 wt% aq nitric acid is a theta solvent for γ-PAN and in that mixture both $[\eta]$ and $\langle S^2\rangle_z^{1/2}$ are proportional to $\bar{M}_w^{1/2}$. (4) In DMSO, A_2 for R-PAN is larger than that for γ-PAN when compared at the same $\bar{M}_w$. (5) The unperturbed chain dimension A is larger for γ-PAN than for R-PAN.

APPENDIX

Derivation of Eq 17 ~ 19

We assume that the polymer chain is an assemble of $E_m(h)$ rigid meso blocks $m_1m_2\cdots m_h$ ($h=1, 2, \cdots, n$) and $E_r(q)$ racemo blocks $r_1r_2\cdots r_q$ ($q=1,2,\cdots, q'$), both arranged linearly. Equation 16 does not change independently of the permutation of the assemble. We define $L(i)=|l_i|$ and rearrange l_i from $i=1$ to $\sum_{h=1}^{n} E_m(h)+D$ in the following manner.

$$L(1)=L(2)=\cdots=L(E_m(1))=b_m$$

$$L(E_m(1)+1)=\cdots=L\left(\sum_{h=1}^{2} E_m(h)\right)=2b_m$$

$$\cdots$$

$$L\left(\sum_{h=1}^{n-1} E_m(h)+1\right)=\cdots=L\left(\sum_{h=1}^{n} E_m(h)\right)=nb_m$$

$$L\left(\sum_{h=1}^{n} E_m(h)+1\right)=\cdots=L\left(\sum_{h=1}^{n} E_m(h)+D\right)=b$$

Then, the first term in the right-hand side of eq 16 can be devided into two parts (see Figure 13):

(i) for $l_i=xb_m$

$$\sum_{x=1}^{n} E_m(x)(xb_m)^2 \qquad (A\cdot 1)$$

(ii) for $l_i=b$

$$\sum_{x=1}^{q'} 2(x\overline{F_r(x)})b^2=Db^2 \qquad (A.2)$$

and the second term in the right-hand side of eq 16 can be devided into four parts:

(iii) for $l_i=l_j=xb_m$ ($x=1, \cdots, n$)

$$
\begin{aligned}
&2\sum_{\substack{i=1\\(i<j)}}^{E_m(1)}\sum_{j=i}^{E_m(1)}(1b_m)(1b_m)(-\cos\theta)^{j-i}\\
&\quad+2\sum_{\substack{i=1\\(i<j)}}^{E_m(2)}\sum_{j=1}^{E_m(2)}(2b_m)(2b_m)(-\cos\theta)^{\{(j+E_m(1))-(i+E_m(1))\}}\\
&\quad+\cdots\\
&\quad+2\sum_{\substack{i=1\\(i<j)}}^{E_m(n)}\sum_{j=1}^{E_m(n)}(nb_m)(nb_m)(-\cos\theta)^{\left\{\left(j+\sum_{h=1}^{n-1}E_m(h)\right)-\left(i+\sum_{h-1}^{n-1}E_m(h)\right)\right\}}\\
&\quad=2\sum_{x=1}^{n}\left\{\sum_{\substack{i=1\\(i<j)}}^{E_m(x)}\sum_{j=1}^{E_m(x)}(xb_m)(-\cos\theta)^{(j-i)}\right\}
\end{aligned}
\tag{A.3}
$$

(iv) for $l_i=l_j=b$

$$
\begin{aligned}
&2\sum_{i=1}^{D}\sum_{j=1}^{D}b\cdot b(-\cos\theta)^{\left\{\left(j+\sum_{h=1}^{n}E_m(h)\right)-\left(i+\sum_{h-1}^{n}E_m(h)\right)\right\}}\\
&\quad=2\sum_{i=1}^{D}\sum_{j=1}^{D}(-\cos\theta)^{(j-i)}
\end{aligned}
\tag{A.4}
$$

(v) for $l_i=xb_m$ and $l_j=yb_m$, $(x<y;\ x,\ y=1,\ \cdots,\ n)$

$$
\begin{aligned}
&2\sum_{i=1}^{E_m(1)}\sum_{j=1}^{E_m(2)}(1b_m)(2b_m)(-\cos\theta)^{(j+E_m(1)-i)}\\
&\quad+\cdots\\
&\quad+2\sum_{i=1}^{E_m(1)}\sum_{j=1}^{E_m(n)}(1b_m)(nb_m)(-\cos\theta)^{\left(j+\sum_{h=1}^{n-1}E_m(h)-i\right)}\\
&\quad+2\sum_{i=1}^{E_m(2)}\sum_{j=1}^{E_m(3)}(2b_m)(3b_m)(-\cos\theta)^{\left\{\left(j+\sum_{h=1}^{3-1}E_m(h)\right)-\left(i+\sum_{h=1}^{2-1}E_m(h)\right)\right\}}\\
&\quad+\cdots\\
&\quad+2\sum_{i=1}^{E_m(2)}\sum_{j=1}^{E_m(n)}(2b_m)(nb_m)(-\cos\theta)^{\left\{\left(j+\sum_{h=1}^{n-1}E_m(h)\right)-\left(i+\sum_{h-1}^{2-1}E_m(h)\right)\right\}}\\
&\quad+\cdots\\
&\quad+2\sum_{i=1}^{E_m(n-1)}\sum_{j=1}^{E_m(n)}\{(n-1)b_m\}(nb_m)(-\cos\theta)^{\left\{\left(j+\sum_{h=1}^{n-1}E_m(h)\right)-\left(i+\sum_{h=1}^{(n-1)-1}E_m(h)\right)\right\}}\\
&\quad=2\sum_{\substack{x=1\\(x<y)}}^{n}\sum_{y=1}^{n}\left\{\sum_{i=1}^{E_m(x)}\sum_{j=1}^{E_m(y)}(xb_m)(yb_m)(-\cos\theta)^{\left(j-i+\sum_{h=x}^{y-1}E_m(h)\right)}\right\}
\end{aligned}
\tag{A.5}
$$

(vi) for $l_i = xb_m$ and $l_j = b$ $(x = 1, \cdots, n)$

$$\sum_{i=1}^{E_m(1)} \sum_{j=1}^{D} b(1b_m)(-\cos\theta)\left(j+\sum_{h=1}^{n} E_m(h)-i\right)$$
$$+\sum_{i=1}^{E_m(2)} \sum_{j=1}^{D} b(2b_m)(-\cos\theta)\left\{\left(j+\sum_{h=1}^{n} E_m(h)\right)-\left(i+\sum_{h=1}^{2-1} E_m(h)\right)\right\}$$
$$+\cdots$$
$$+\sum_{i=1}^{E_m(n)} \sum_{j=1}^{D} b(nb_m)(-\cos\theta)\left\{\left(j+\sum_{h=1}^{n} E_m(h)\right)-\left(i+\sum_{h=1}^{n-1} E_m(h)\right)\right\}$$
$$=\sum_{x=1}^{p}\left\{\sum_{i=1}^{E_m(x)} \sum_{j=1}^{D} b(xb_m)(-\cos\theta)\left(j-i+\sum_{h=x}^{n} E_m(h)\right)\right. \tag{A.6}$$

Summation of eq A·1 ~eq A·6 gives eq 17. By putting $n=p'$ in eq 19a and 19b, we obtain $E_m(h)=\bar{F}_m(h)$ and, by putting $k'\to\infty$ $(p'\to\infty)$, we obtain $\overline{F_m(p')}\to 0$. In the case of $k'\to\infty$, eq 19a and 19b reduces to

$$E_m(h)=\sum_{k=0}^{\infty} \overline{F_m(kp+h)} \qquad (h=1, \cdots, p) \tag{A·7}$$

REFERENCES

1. J. B. Kinsinger and R. E. Hughes, *J. Phys. Chem.*, **63**, 2002 (1959).
2. P. Parrini, F. Sebastiano, and G. Messina, *Makromol. Chem.*, **38**, 27 (1960).
3. J. B. Kinsinger and R. E. Hughes, *J. Phys. Chem.*, **67**, 1922 (1963).
4. H. Inagaki, T. Miyamoto, and S. Ohta, *J. Phys. Chem.*, **70**, 3420 (1966).
5. A. Nakajima and A. Saigo, *J. Polym. Sci.*, **6**, 735 (1968).
6. I. Sakurada, A. Nakajima, O. Yoshizaki, and K. Nakamae, *Kolloid Z.-Z. Polym. B*, **186**, 41 (1962).
7. S. Krause and E. Cohn-Ginsberg, *Polymer*, **3**, 565 (1962).
8. S. Krause and E. Cohn-Ginsberg, *J. Phys. Chem.*, **67**, 1479 (1963).
9. G. V. Schulz, W. Wunderlich, and R. Kirste, *Makromol. Chem.*, **75**, 22 (1964).
10. F. Danusso and G. Moraglio, *J. Polym. Sci.*, **24**, 161 (1957).
11. W. R. Krigbaum, D. K. Capenter, and S. Newman, *J. Phys. Chem.*, **62**, 1586 (1958).
12. L. Trossarelli, E. Campi, and G. Saini, *J. Polym. Sci.*, **35**, 205 (1959).
13. J. M. G. Cowie, B. Bywater, and D. J. Worsfold, *Polymer*, **8**, 105 (1967).
14. J. M. G. Cowie and S. Bywater, *J. Polym. Sci.*, **6**, 499 (1968).
15. T. Kato, K. Miyaso, I. Noda, T. Fujimoto, and M. Nagasawa, *Macromolecules*, **3**, 777 (1970).
16. T. Kato, K. Miyaso, I. Noda, T. Fujimoto, and M. Nagasawa, *Macromolecules*, **3**, 787 (1970).
17. W. R. Krigbaum, J. E. Kurz, and P. Smith, *J. Phys. Chem.*, **65**, 1984 (1961).
18. K. Satynarayana, S. Astry, and R. D. Patel, *Eur. Polym. J.*, **5**, 79 (1969).
19. G. Moraglio and J. Brzezinski, *J. Polym. Sci., B*, **2**, 1105 (1964).
20. G. Moraglio and G. Gianotti, *Eur. Polym. J.*, **5**, 781 (1969).
21. J. E. Mark, R. A. Wessling, and R. E. Hughes, *J. Phys. Chem.*, **70**, 1895 (1966).
22. J. E. Mark, R. A. Wessling, and R. E. Hughes, *J. Phys. Chem.*, **70**, 1903 (1966).
23. M. Matsumoto and Y. Ohyanagi, *J. Polym. Sci.*, **37**, 558 (1959).
24. K. Kamide, *Kobunshi*, **11**, 49 (1962).
25. W. R. Krigbaum, "Newer Method of Polymer Characterization," B. Ke, Ed., John Willey & Sons, New York, N. Y., 1964, Chapter 1.
26. J. M. G. Cowie "Light Scattering from Polymer Solution," M. B. Huglin, Ed., Academic Press, New York, N. Y., 1972, Chapter 14.
27. H. Inagaki, K. Hayashi, and T. Matsuo, *Makromol. Chem.*, **84**, 80 (1965).
28. K. Kamide and T. Terakawa, *Makromol. Chem.*, **155**, 25 (1972).
29. K. Matsuzaki, T. Uryu, M. Okada, and H. Shiroki, *J. Polym. Sci., A-1*, **6**, 1475 (1968).

30. K. Matsuzaki, T. Uryu, M. Okada, and H. Shiroki, *J. Polyn. Sci., A-1*, **9**, 1701 (1971).
31. K. Kamide, H. Kobayashi, Y. Miyazaki, and C Nakayama, *Kobunshi Kagaku*, **24**, 679 (1967).
32. K. Kamide, H. Yamazaki, K. Okajima, and K. Hikichi, *Polym. J.*, **17**, 1233 (1985).
33. K. Kamide, H. Yamazaki, K. Okajima, and K. Hikichi, *Polym. J.*, **17**, 1291 (1985).
34. D. M. White, *J. Am. Chem. Soc.*, **82**, 5678 (1960).
35. K. Kamide, Y. Miyazaki, and H. Kobayashi, *Polym. J.*, **17**, 607 (1985).
36. Y. Fujisaki and H. Kobayashi, *Kobunshi Kagaku*, **19**, 49 (1962).
37. H. Yamazaki, K. Kamide, and Y. Miyazaki, to be submitted to *Polym. J.*
38. M. Kurata, M. Fukatsu, H. Sotobayashi, and H. Yamakawa, *J. Chem. Phys.*, **41**, 139 (1964).
39. M. Fixman, *J. Chem. Phys.*, **36**, 3123 (1962).
40. H. Baumann, *J. Polym. Sci., Polym. Lett. Ed.*, **3**, 1069 (1965).
41. W. H. Stockmayer and M. Fixman, *J. Polym. Sci., C*, **1**, 137 (1963).
42. K. Kamide and W. Moore, *J. Polym. Sci., Polym. Lett. Ed.*, **2**, 1029 (1964).
43. M. Kurata, Y. Tsumashima, M. Iwata, and K. Kamata, "Polymer Handbook," 2nd ed, J. Brandrup and E. H. Immergut, Ed., John Wiley & Sons, New York, N. Y., 1975.
44. A. Dondos and H. Benoit, *Macromolecules*, **4**, 279 (1971).
45. K. Kamide, H. Yamazaki, K. Okajima, and K. Hikichi, *Polym.J.*, **18**, 277 (1986).